

# Electronic Supplementary Information

## Synthesis of aminyl biradicals by base-induced Csp<sup>3</sup>–Csp<sup>3</sup> coupling of cationic azo dyes

Yizhu Liu,<sup>a</sup> Paul Varava,<sup>a</sup> Alberto Fabrizio,<sup>a</sup> Leonard Y. M. Eymann,<sup>a</sup> Alexander G. Tskhovrebov,<sup>a</sup>  
Ophélie Marie Planes,<sup>a</sup> Euro Solari,<sup>a</sup> Farzaneh Fadaei-Tirani,<sup>a</sup> Rosario Scopelliti,<sup>a</sup> Andrzej  
Sienkiewicz,<sup>b</sup> Clémence Corminboeuf,<sup>a</sup> and Kay Severin<sup>a\*</sup>

<sup>a</sup> Institut des Sciences et Ingénierie Chimiques, École Polytechnique Fédérale de Lausanne (EPFL), CH-1015 Lausanne, Switzerland

<sup>b</sup> Institute of Physics, École Polytechnique Fédérale de Lausanne (EPFL), CH-1015 Lausanne, Switzerland

### Contents

1. Synthetic procedures.....	S2
2. NMR spectra .....	S5
3. ESR spectroscopy .....	S16
4. X-Ray crystallography.....	S18
5. Cyclic voltammetry of compound <b>4</b> .....	S20
6. DFT computations .....	S21

## 1. Synthetic procedures

### General

Unless stated otherwise, the reactions were performed under an atmosphere of dry dinitrogen using either a dinitrogen-filled glovebox or Schlenk techniques. Solvents (pentane, hexane, toluene, chlorobenzene, THF, dichloromethane) were dried with the Innovative Technology SPS-400-5 solvent purification system. (2,2,6,6-Tetramethylpiperidin-1-yl)oxyl (TEMPO, FluoroChem) was vacuum sublimed before use. Potassium bis(trimethylsilyl)amide (KHMDs, Sigma Aldrich), lithium bis(trimethylsilyl)amide (LiHMDS, Sigma Aldrich), mesitylene (Acros), and AlCl<sub>3</sub> (Acros) were commercially available and used as received. Compounds **1**,<sup>1</sup> **5**<sup>2</sup> and **10**<sup>2</sup> were prepared according to literature.

The original data files for this manuscript can be found at DOI:10.5281/zenodo.2669473 (<https://zenodo.org/record/2669473#.XNBZj45LguU>)

**Preparation of 3.** Compound **1** (114 mg, 0.21 mmol) was dissolved in THF (20 mL), and the resulting bright orange solution was cooled in the cold well of a glovebox which was immersed in a bath of liquid nitrogen. After the flask was well cooled, a THF (3 mL) solution of KHMDs (42.4 mg, 0.21 mmol) was carefully dropped inside using a pipette, and the resulting mixture was allowed to warm up while shielded from direct light irradiation. Substantial darkening of the solution occurred after the flask reached room temperature, and after 4 h stirring, a dark rose-brown solution was obtained. The solvent was pumped off at this stage, and the solid residue was washed with pentane (ca. 6 mL). The remaining crude product was extracted with toluene (6 mL) and filtered into a test tube (Ø 1 cm × 10 cm), to which a vapor of pentane was allowed to slowly diffuse at –40 °C. After 20 days, the mother liquid was carefully removed using a pipette, and the resulting black crystals were washed with cold pentane to give compound **3**. Yield: 40 mg (42%). Crystals suitable for X-ray diffraction crystallography were obtained by cooling a saturated THF–pentane solution of **3** at –40 °C overnight. ESR *g*-factor: 2.0037. Due to the low stability of the biradical **3**, further analytical characterization was not achieved.

**Preparation of 4.** A solution of KO<sup>t</sup>Bu (26.1 mg, 0.23 mmol, 1 eq.) in THF (10 mL) was added over a period of 1 h to a cooled (–78 °C) solution of compound **1** (125 mg, 0.23 mmol, 1 eq.) in THF (30 mL). The color changed from orange-red to green-yellow. Subsequently, a solution of TEMPO (36.3 mg, 0.23 mmol, 1 eq.) in THF (5 mL) was added over a period of 30 min. Cooling was stopped after 1 h, and the solution was stirred overnight, slowly becoming blue. The next day, the solvent was removed under reduced pressure, and the residue was dried for 3 h. After thorough washing with cyclohexane and drying, the solid was redissolved in THF, filtered, and the THF was removed under reduced pressure. The resulting solid was washed with DMSO, until the DMSO appeared clear. The product was washed extensively with hexane and pentane, and then it was dried for 2 d using a diffusion pump. Yield: 59 mg (71%). Crystals suitable for X-ray diffraction crystallography were obtained by slow diffusion of pentane into a solution of **3** in chlorobenzene at room

<sup>1</sup> A. G. Tskhovrebov, L. C. E. Naested, E. Solari, R. Scopelliti and K. Severin. *Angew. Chem. Int. Ed.*, 2015, **54**, 1289–1292.

<sup>2</sup> L. Y. M. Eymann, R. Scopelliti, F. Fadaei Tirani and K. Severin. *Chem. Eur. J.*, 2018, **24**, 7957–7963.

temperature over several days.  $^1\text{H}$  NMR (THF- $d_8$ , 25 °C,  $\delta$  ppm) 6.93 (s, 8H, *m*-Mes), 6.59 (s, 4H,  $\text{CH}_{\text{imidazole}}$ ), 6.29 (s, 2H, central C=CH), 5.99 (s, broad, 4H,  $\text{C}_6\text{H}_2(\text{CH}_3)_2$ ), 2.28 (s, 12H, *p*-Mes), 2.16 (s, 24H, *o*-Mes), 1.87 (s, broad, 6H,  $\text{C}_6\text{H}_2(\text{CH}_3)_2$ ), 1.05 (s, broad, 6H,  $\text{C}_6\text{H}_2(\text{CH}_3)_2$ );  $^{13}\text{C}$  NMR (THF- $d_8$ , 25 °C,  $\delta$  ppm) 150.58, 148.84, 138.28, 136.42, and 134.11 ( $\text{C}_{\text{quart}}$ ), 129.46 (*m*-Mes), 122.42 (central C=CH), 117.03 ( $\text{CH}_{\text{imidazole}}$ ), 21.12 ( $\text{CH}_3$ , *p*-Mes), 18.28 ( $\text{CH}_3$ , *o*-Mes); ESI-MS for singly protonated  $[\text{C}_{60}\text{H}_{66}\text{N}_8]^+$   $m/z$  calc. 898.5410, found 898.5406

**Note:** Due to hindered rotation, the NMR signals of the bridging  $\text{C}_6\text{H}_2(\text{CH}_3)_2$  groups are very broad ( $^1\text{H}$ ) or not detected ( $^{13}\text{C}$ ).

**Preparation of 6 and crystallization of 7.** Compound **5** (70 mg, 0.13 mmol) was dissolved in THF (20 mL), and the resulting bright orange solution was cooled in the cold well of a glovebox which was immersed in a bath of liquid nitrogen. After the flask was well cooled, a THF (3 mL) solution of KHMDS (50.4 mg, 0.25 mmol) was carefully dropped inside using a pipette, and the resulting mixture was allowed to warm up while shielded from direct light irradiation. Substantial darkening of the solution occurred after the flask reached room temperature, and after 5 h stirring, a dark yellow-brown solution was obtained. The solvent was pumped off at this stage, and the solid residue was washed generously with pentane and toluene. The remaining crude product was extracted with THF (3 mL) and filtered into a test tube ( $\varnothing$  1 cm  $\times$  10 cm), to which a vapor of pentane was allowed to slowly diffuse at  $-40$  °C. After 30 days, the mother liquid was carefully removed using a pipette, and the obtained dark yellow-brown crystals were washed with cold pentane to give compound **6**. Yield: 23 mg (36%). Crystals suitable for X-ray diffraction crystallography were obtained in the same way. ESR  $g$ -factor: 2.0036. Due to the low stability of the biradical **6**, further analytical characterization was not achieved.

When the above-mentioned crystallization was performed *at room temperature under air*, red crystals of **7** were obtained (see main text).

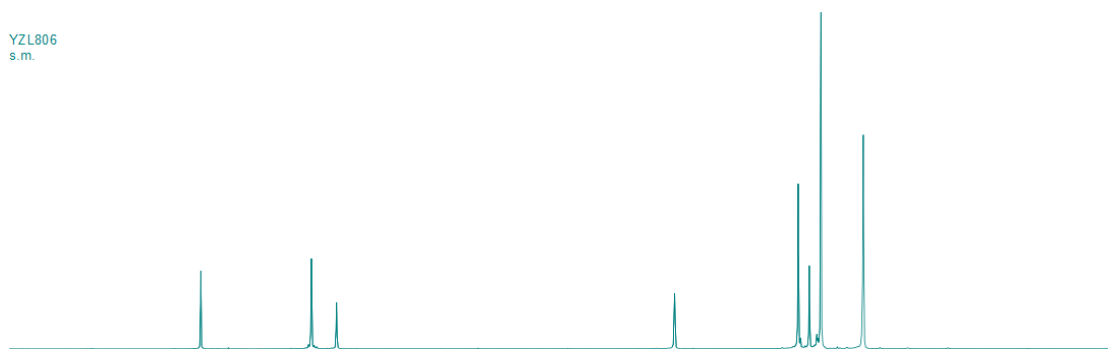
**Preparation of 11.** Compound **10** (266 mg, 0.73 mmol) was suspended in THF (20 mL), and a THF (5 mL) solution of LiHMDS (134 mg, 0.8 mmol) was slowly dropped inside using a pipette to yield a dark brown solution. After stirring for 30 min, the mixture was filtered and evaporated to dryness. The residue was re-dissolved in THF (2 mL), filtered, and triturated with hexane overnight. The precipitates were collected by filtration and dried to give compound **11** as a beige powder. Yield: 286 mg (92%). Crystals suitable for X-ray diffraction crystallography were obtained by layering a THF solution of **11** with pentane at  $-40$  °C.  $^1\text{H}$  NMR (THF- $d_8$ , 25 °C,  $\delta$  ppm) 8.10 (d, 2H,  $J=7.6$  Hz, *o*-Ph), 7.35 (t, 1H,  $J=7.6$  Hz, *p*-Dipp), 7.26 (t, 2H,  $J=7.6$  Hz, *m*-Ph), 7.20 (d, 2H,  $J=7.6$  Hz, *m*-Dipp), 7.15 (t, 1H,  $J=7.4$  Hz, *p*-Ph), 2.48 (sept, 2H,  $J=6.8$  Hz,  $\text{CHMe}_2$ ), 1.08 (dd, 12H,  $J=12.2, 7.0$  Hz,  $\text{CH}(\text{CH}_3)_2$ );  $^{13}\text{C}$  NMR (THF- $d_8$ ,  $\delta$  ppm) 147.11 (*o*-Dipp), 144.72 (5-triazole), 135.04 (*ipso*-Dipp), 135.01 (4-triazole), 133.90 (*ipso*-Ph), 130.21 (*p*-Dipp), 128.26 (*m*-Ph), 127.26 (*o*-Ph), 126.84 (*p*-Ph), 123.69 (*m*-Dipp), 29.27 ( $\text{CHMe}_2$ ), 24.53 ( $\text{CH}(\text{CH}_3)_2$ ), 22.99 ( $\text{CH}(\text{CH}_3)_2$ ). ESI-MS for doubly protonated  $[\text{C}_{20}\text{H}_{24}\text{N}_5\text{O}]^+$   $m/z$  calc. 350.1981, found 350.1975.

**Preparation of 12.** Compound **11** (139 mg, 0.33 mmol) and an excess of mesitylene (ca. 1.5 mL) were dissolved in DCM (15 mL), and the solution was cooled down to  $-78$  °C.  $\text{AlCl}_3$  (130 mg, 0.98 mmol) was added against a nitrogen flux and the mixture was stirred for 5 min before the

cooling bath was removed. The flask was allowed to warm to room temperature and stirred for 2.5 h. The solvent was then removed under vacuum and the residue was extracted with DCM and filtered. The DCM phase was brought to dryness, and the residue was re-precipitated with DCM/hexane. The solid product was collected by filtration to give compound **12** as an orange powder. Yield: 97 mg (65%).  $^1\text{H}$  NMR (THF- $d_8$ , 25°C,  $\delta$  ppm) 8.29 (d, 2H,  $J=7.2$  Hz, *o*-Ph), 7.48 – 7.44 (m, 3H, *p*-Dipp & *m*-Ph), 7.39 (t, 1H,  $J=7.4$  Hz, *p*-Ph) 7.32 (d, 2H,  $J=8.0$  Hz, *m*-Dipp), 6.86 (s, 2H, mesityl), 2.36 (sept, 2H,  $J=6.8$  Hz,  $\text{CHMe}_2$ ), 2.24 (s, 3H, *p*-Me<sup>mesityl</sup>), 2.00 (s, 6H, *o*-Me<sup>mesityl</sup>), 1.12 (d, 6H,  $J=6.8$  Hz,  $\text{CH}(\text{CH}_3)_2$ ), 0.99 (d, 6H,  $J=6.8$  Hz,  $\text{CH}(\text{CH}_3)_2$ );  $^{13}\text{C}$  NMR (THF- $d_8$ ,  $\delta$  ppm) 148.66 (*ipso*-mesityl), 145.93 (*o*-Dipp), 144.75 (5-triazole), 143.85 (4-triazole), 142.12 (*p*-mesityl), 135.53 (*ipso*-Dipp), 134.67 (*o*-mesityl), 131.49 (*ipso*-Ph), 131.15 (*m*-mesityl), 130.74 (*p*-Dipp), 129.36 (*m*-Dipp), 128.97 (*p*-Ph), 128.71 (*o*-Ph), 124.64 (*m*-Dipp), 29.54 ( $\text{CHMe}_2$ ), 24.59 ( $\text{CH}(\text{CH}_3)_2$ ), 22.67 ( $\text{CH}(\text{CH}_3)_2$ ), 20.99 (*p*-Me<sup>mesityl</sup>), 20.41 (*o*-Me<sup>mesityl</sup>). ESI-MS for singly protonated  $[\text{C}_{29}\text{H}_{34}\text{N}_5]^+$   $m/z$  calc. 452.2814, found 452.2816.

## 2. NMR spectra

YZL806  
s.m.



YZL806  
KHMDS addition

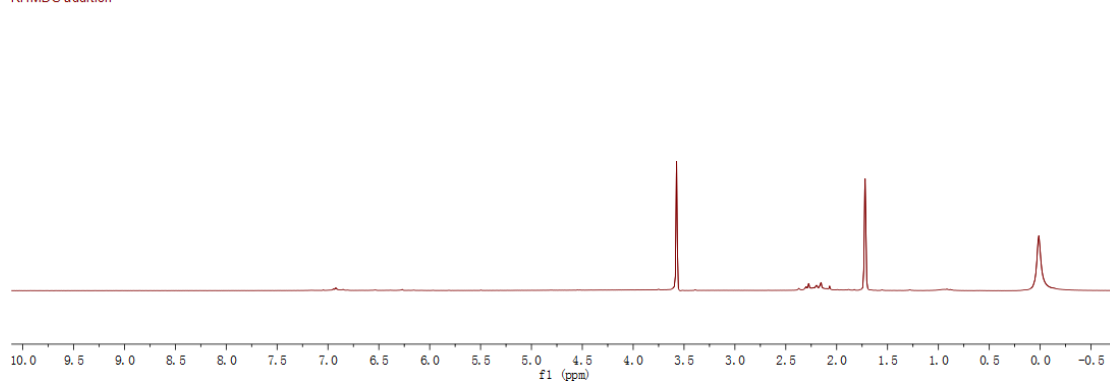


Figure S1  $^1\text{H}$  NMR spectra of **1** in  $\text{THF-d}_8$  before (up) and after (down) addition of KHMDS.

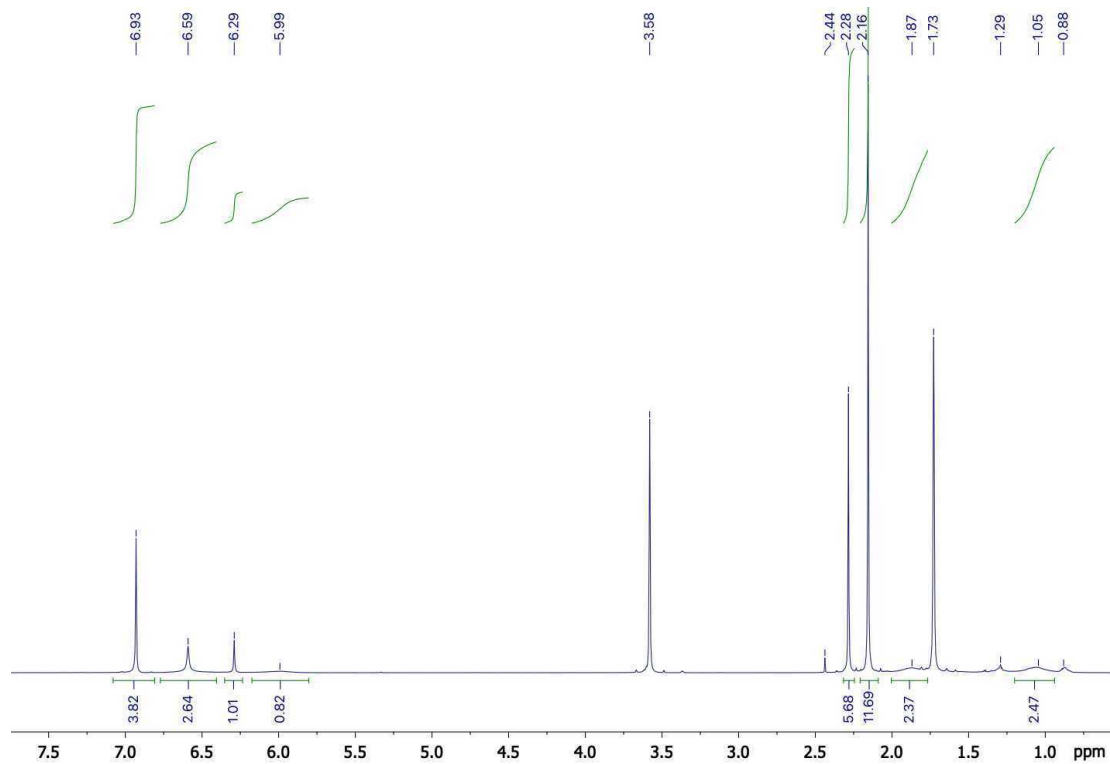


Figure S2  $^1\text{H}$  NMR spectrum of **4** in  $\text{THF-d}_8$ . Due to hindered rotation, the NMR signals of the bridging  $\text{C}_6\text{H}_2(\text{CH}_3)_2$  groups are very broad.

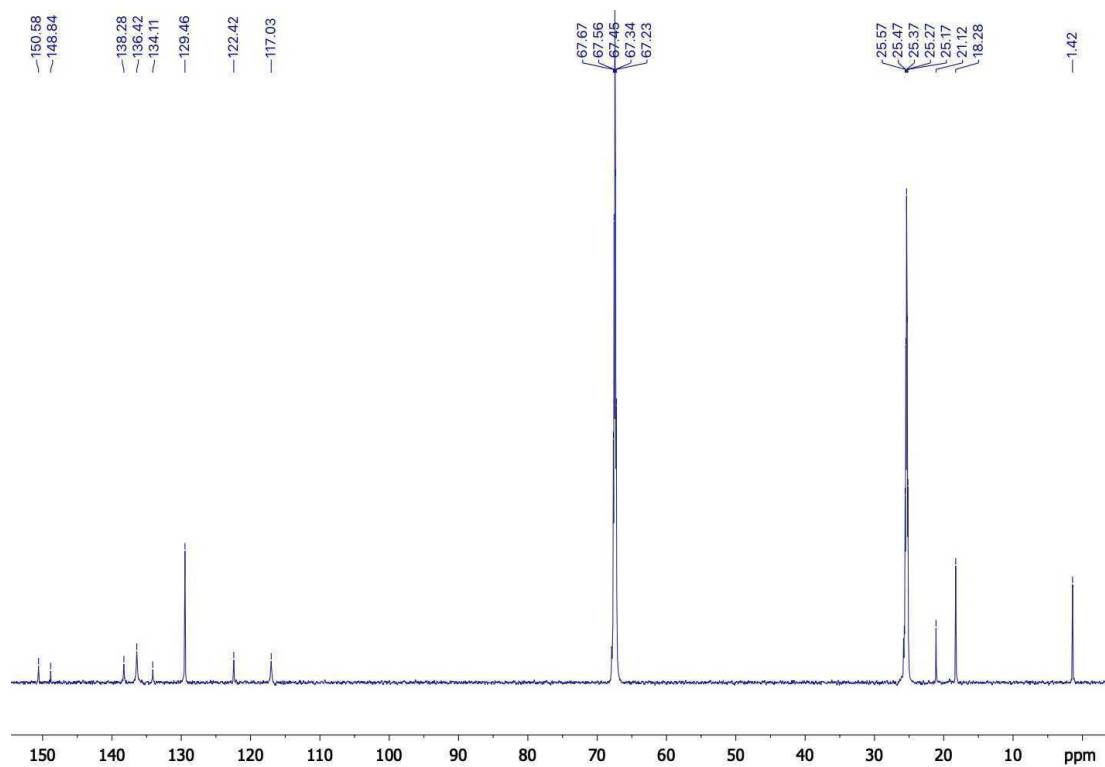


Figure S3  $^{13}\text{C}$  NMR spectrum of **4** in  $\text{THF-d}_8$ . Due to hindered rotation, the NMR signals of the bridging  $\text{C}_6\text{H}_2(\text{CH}_3)_2$  groups are not detected.

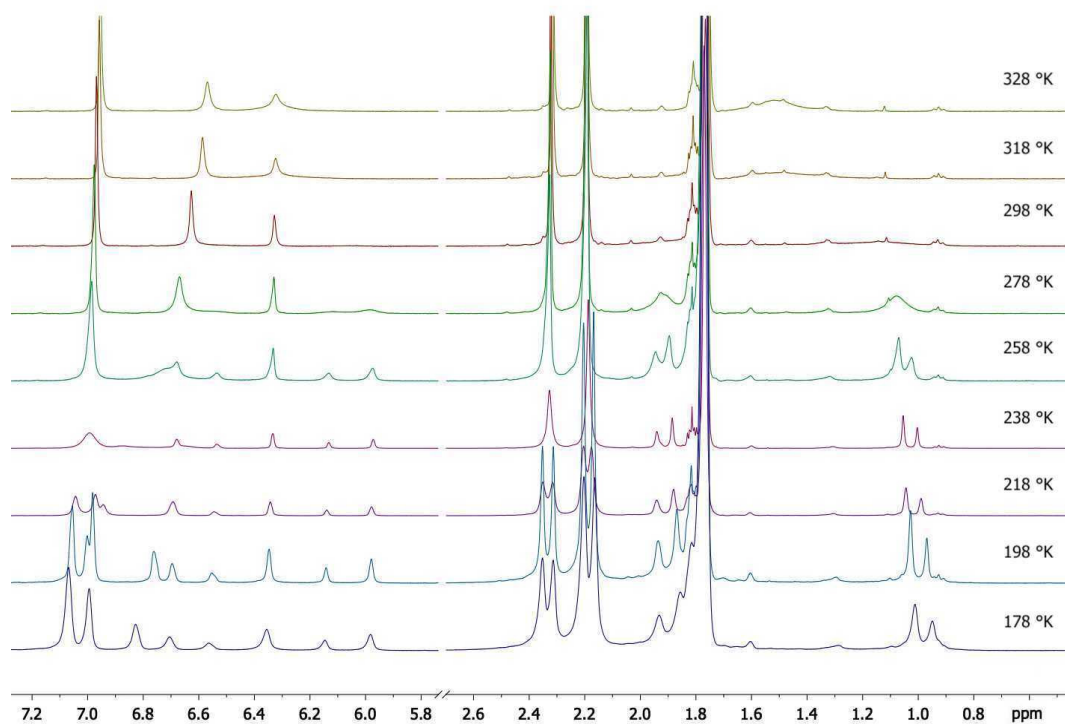


Figure S4 Variable temperature  $^1\text{H}$  NMR spectra of **4** in  $\text{THF-d}_8$ .

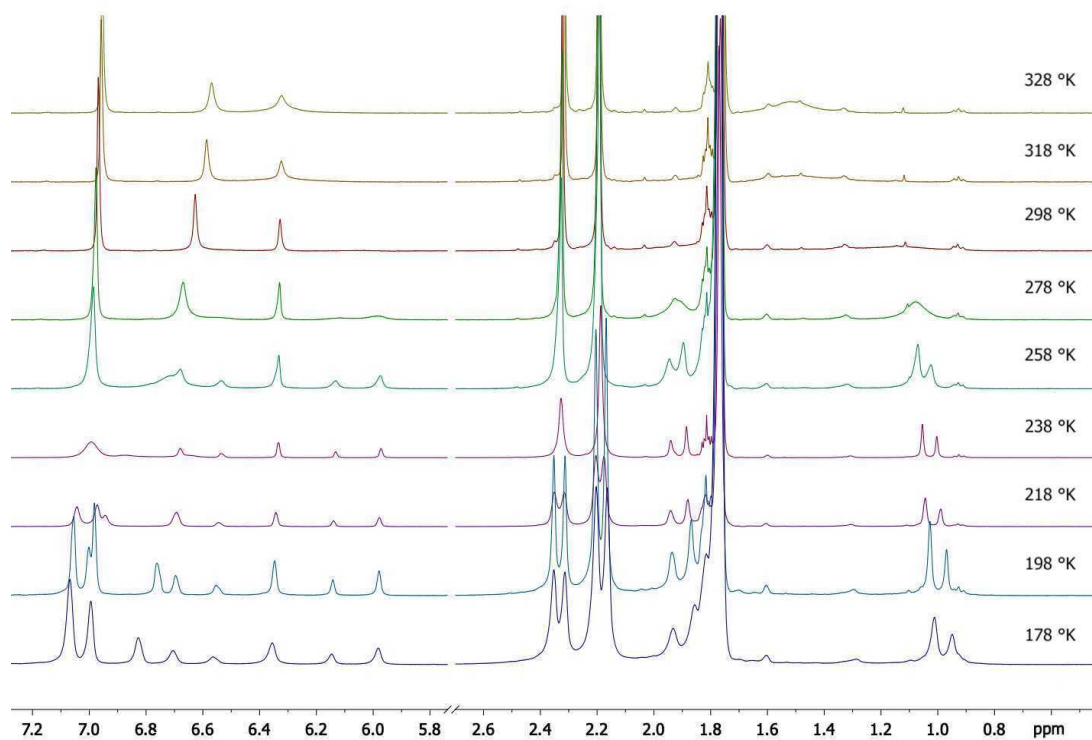


Figure S5 Variable temperature  $^1\text{H}$  NMR spectra of **4** in  $\text{toluene-d}_8$ .

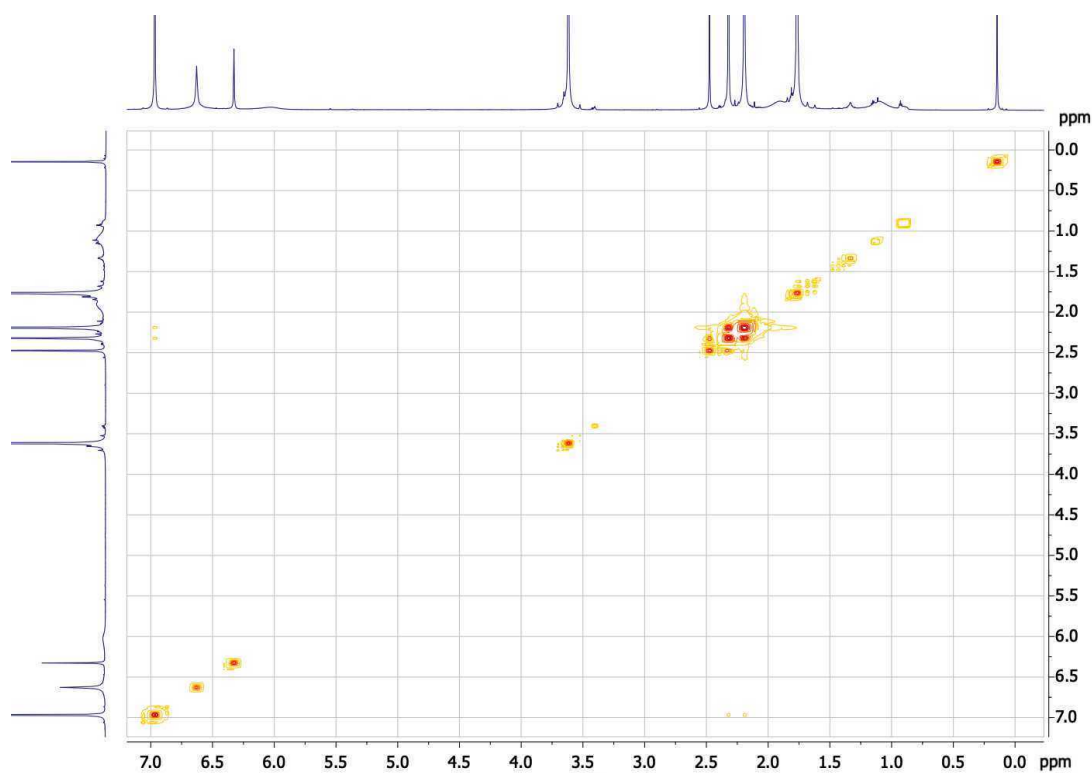


Figure S6 COSY NMR spectrum of **4** in  $\text{THF-d}_8$ .

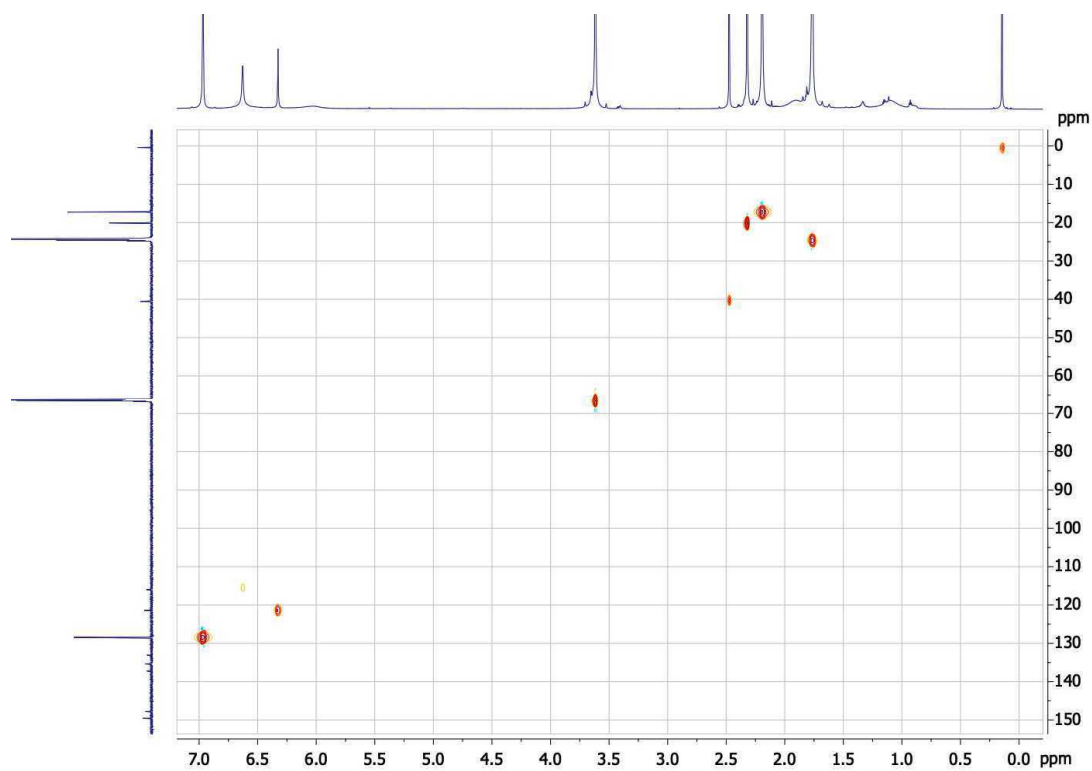


Figure S7 HSQC NMR spectrum of **4** in THF- $d_8$ .

YZL791  
starting tzN2MesBF4

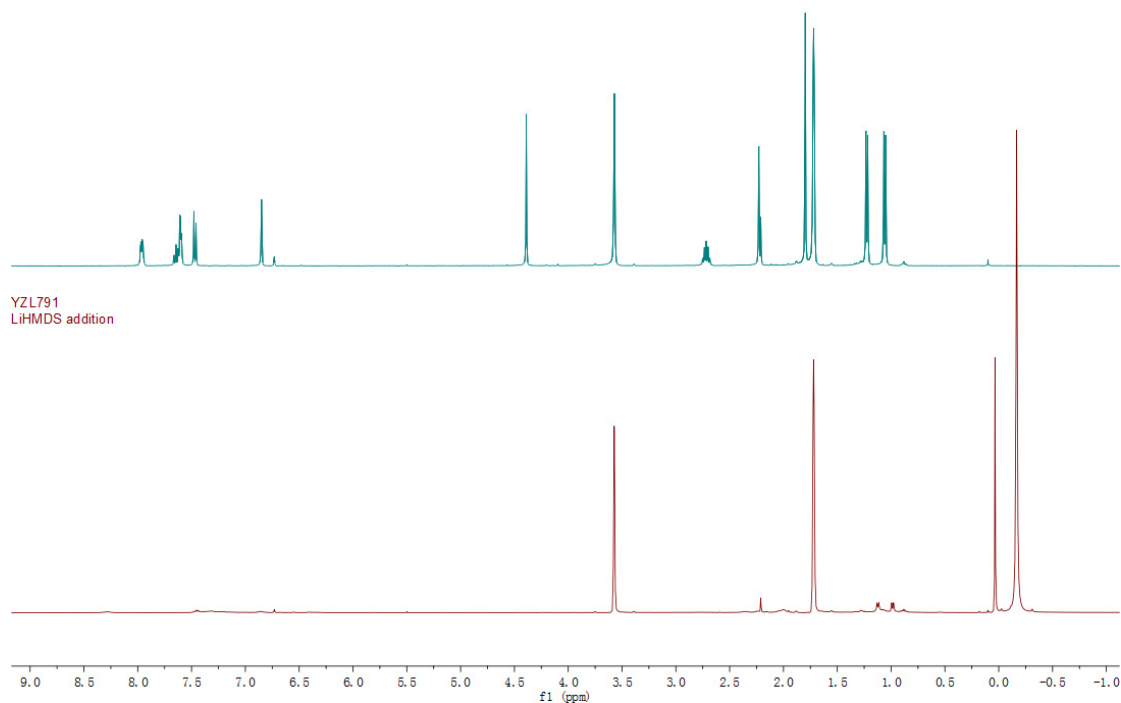


Figure S8  $^1\text{H}$  NMR spectra of **5** in THF- $d_8$  before (up) and after (down) addition of LiHMDS.

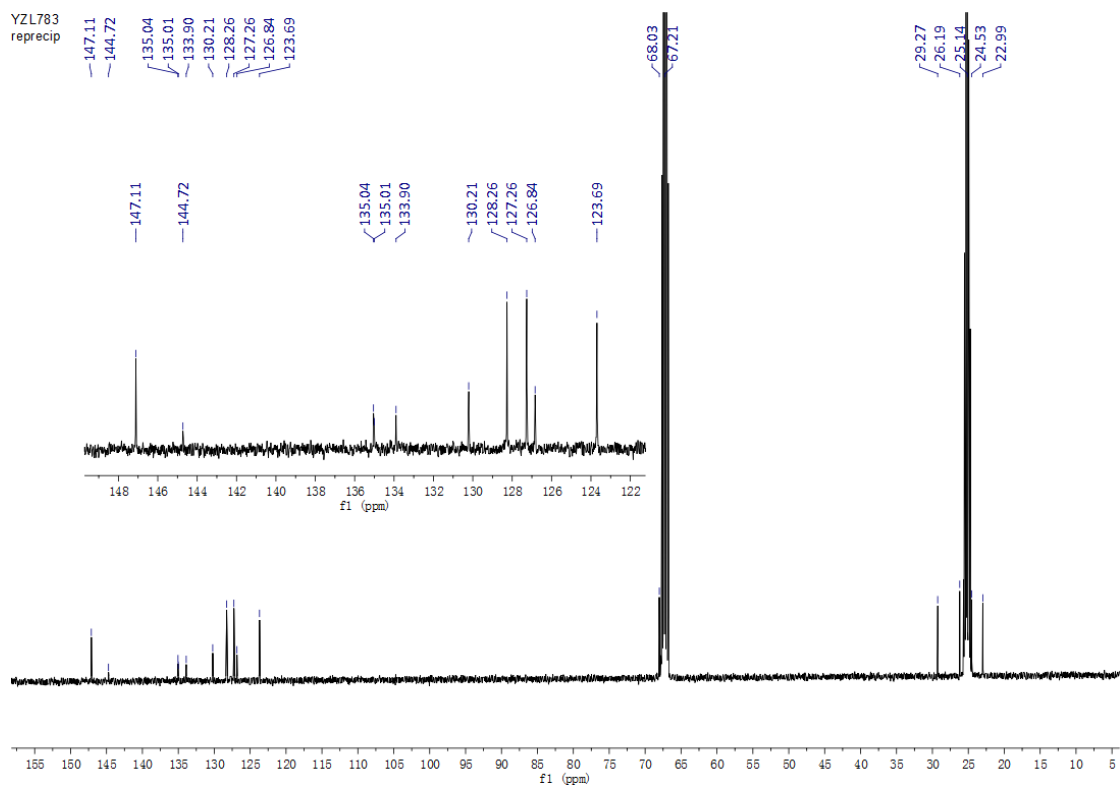
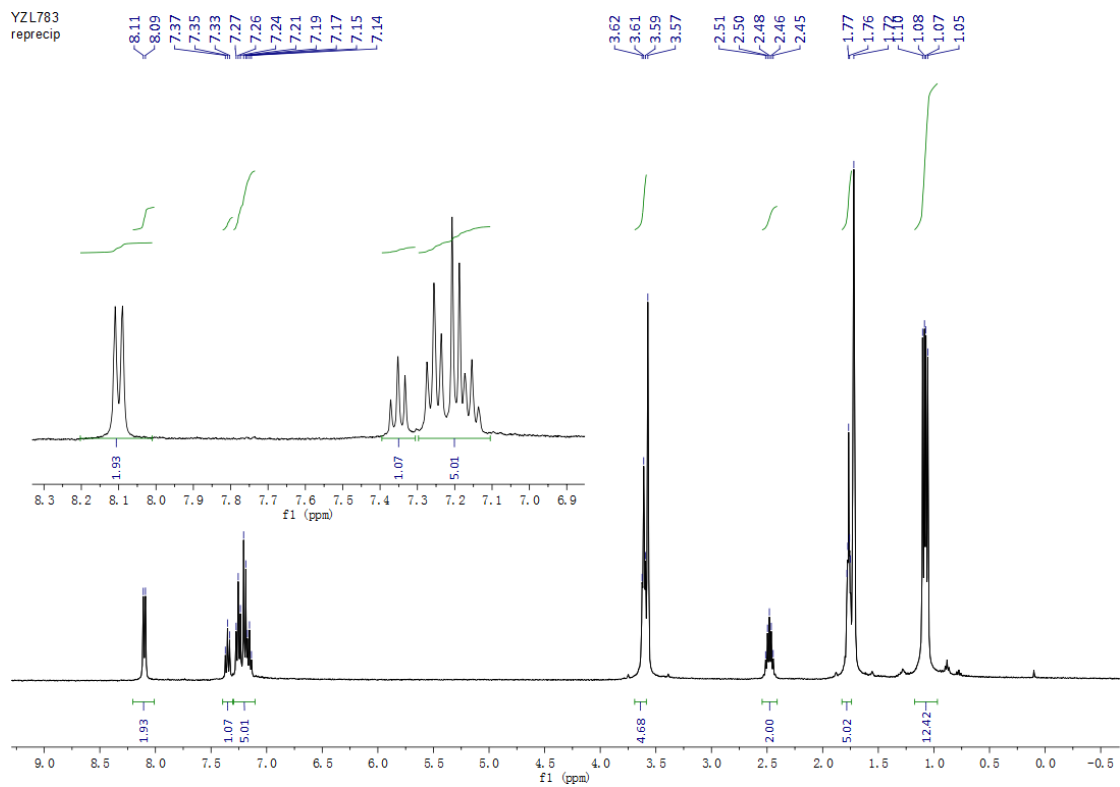


Figure S9  $^1\text{H}$  (top) and  $^{13}\text{C}$  (down) NMR spectra of **11** in  $\text{THF-d}_8$ .

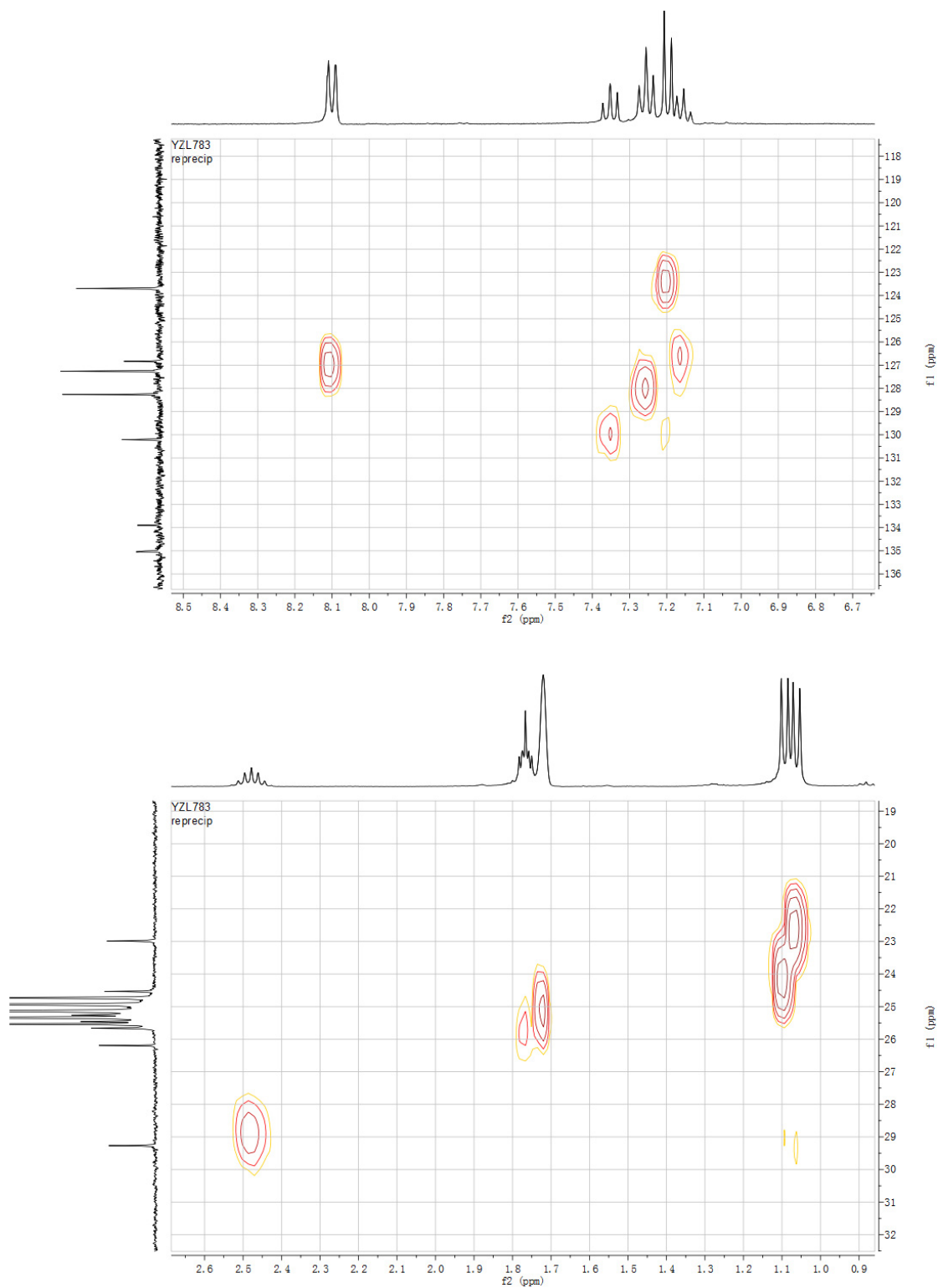


Figure S10 HSQC spectra of **11** in THF-d<sub>8</sub> in the aromatic (top) and aliphatic (down) regions.

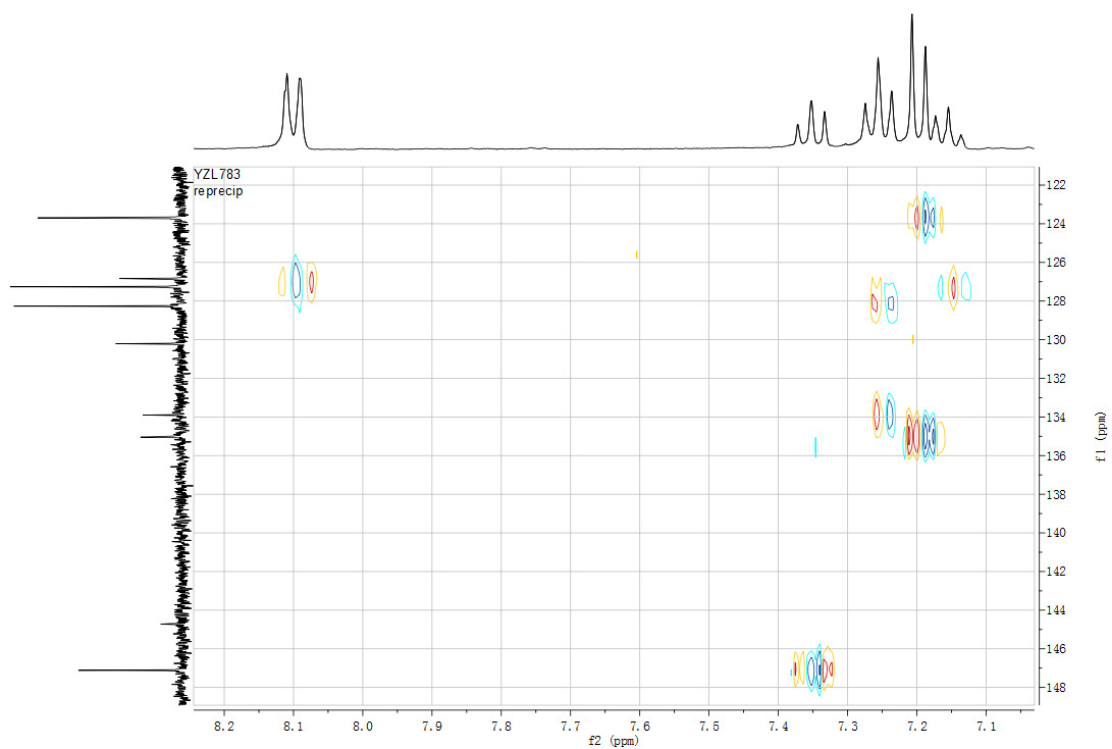
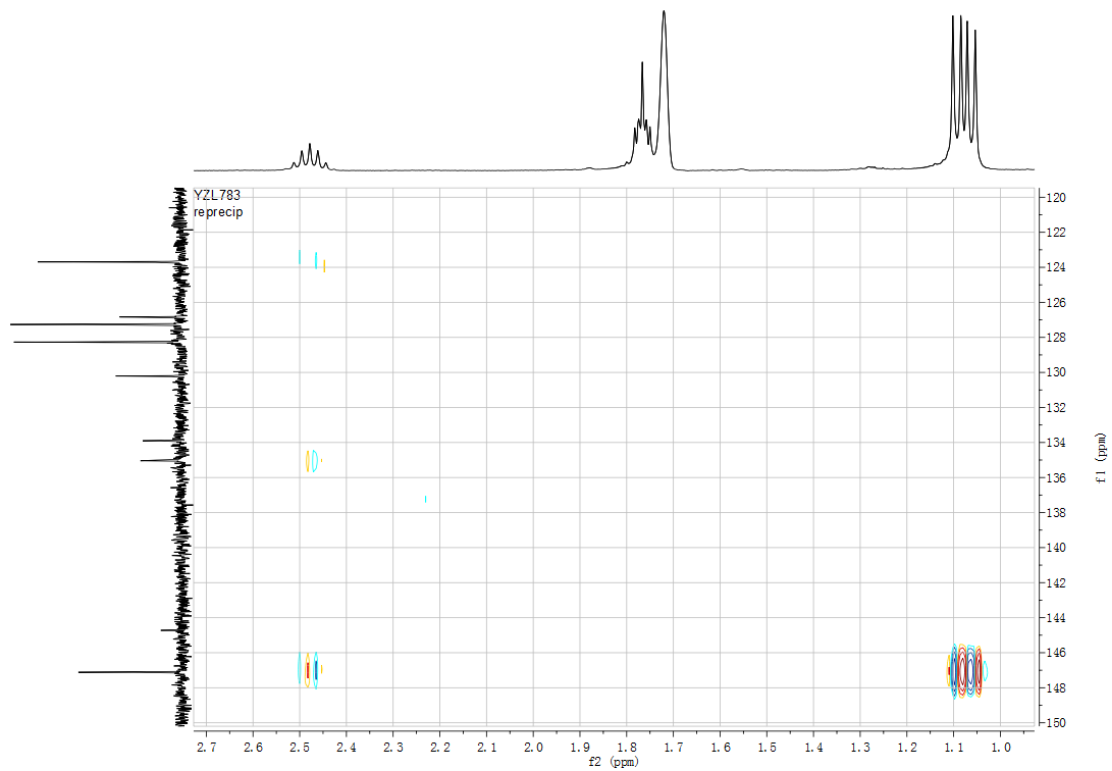


Figure S11 HMBC spectra of **11** in THF- $d_8$ .

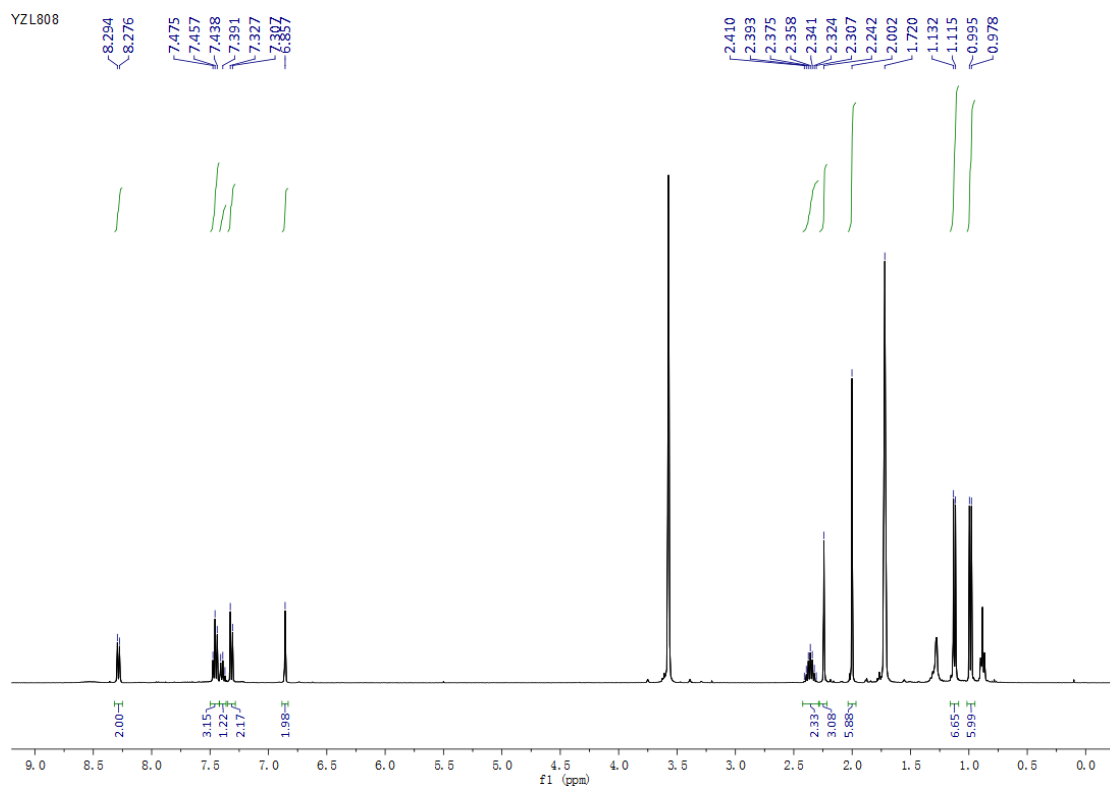


Figure S12  $^1\text{H}$  NMR spectrum of **12** in  $\text{THF-d}_8$ .

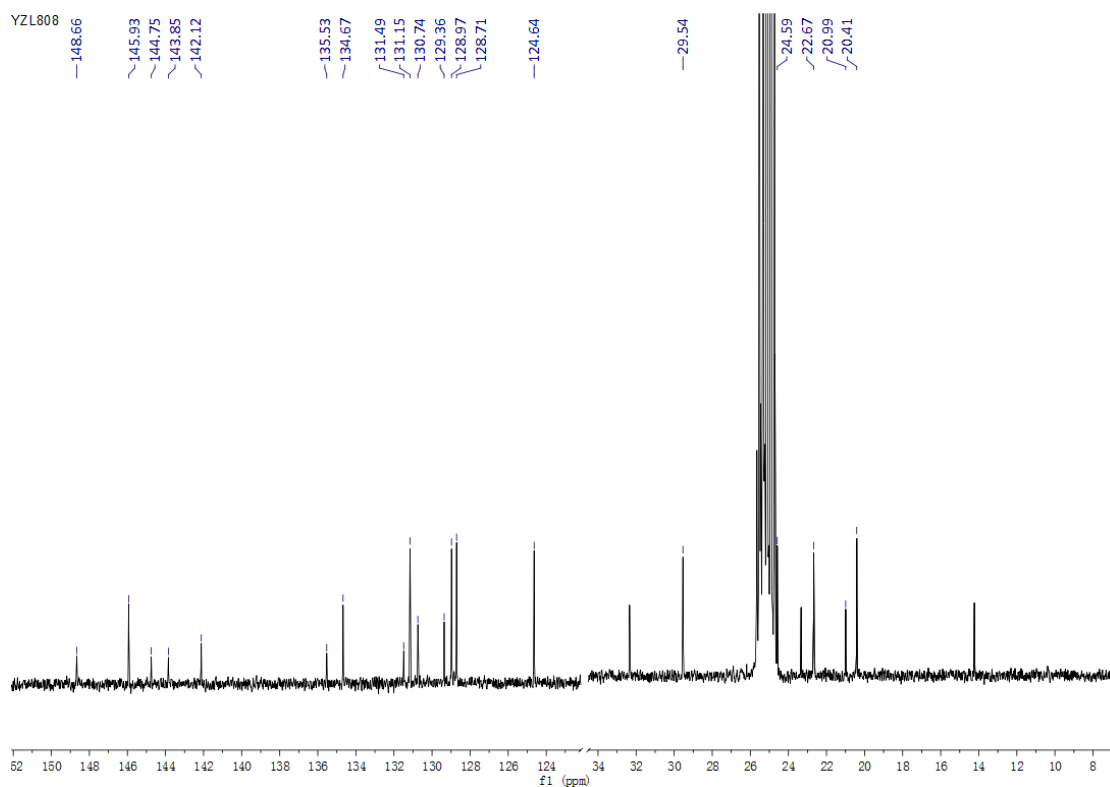


Figure S13  $^{13}\text{C}$  NMR spectrum of **12** in  $\text{THF-d}_8$ . The region containing no peaks of the sample was cut for clarity.

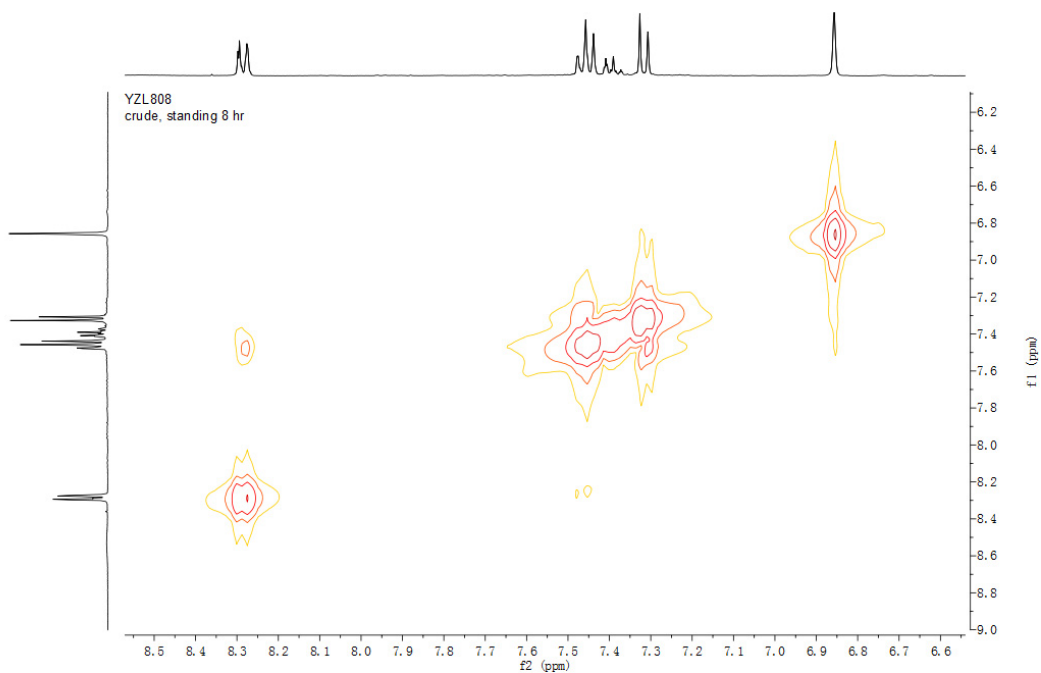


Figure S14 The aromatic region of the COSY spectrum of **12** in THF-d<sub>8</sub>.

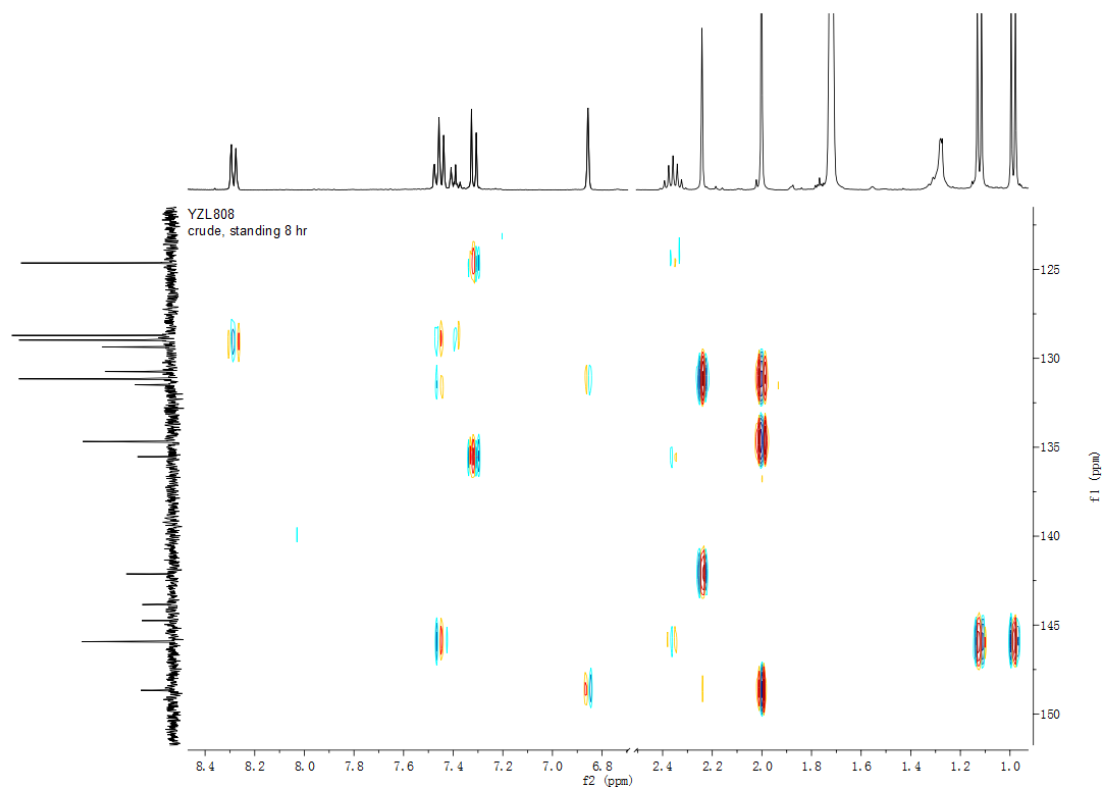


Figure S15 HMBC spectrum of **12** in THF-d<sub>8</sub> showing only the aromatic region on the <sup>13</sup>C axis.

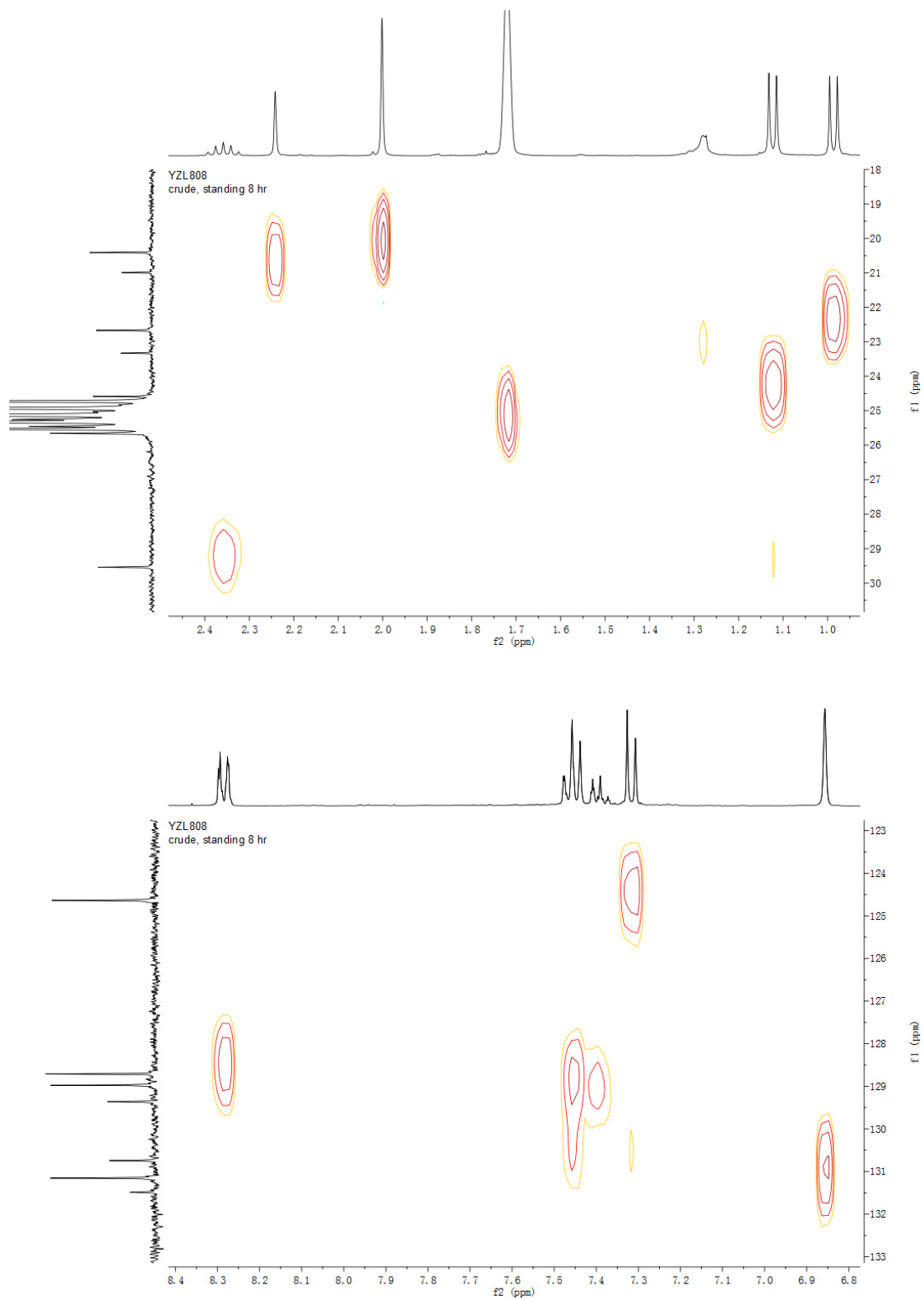


Figure S16 The HSQC spectra of **12** in THF-d<sub>8</sub> in the aliphatic (up) and aromatic (down) regions.

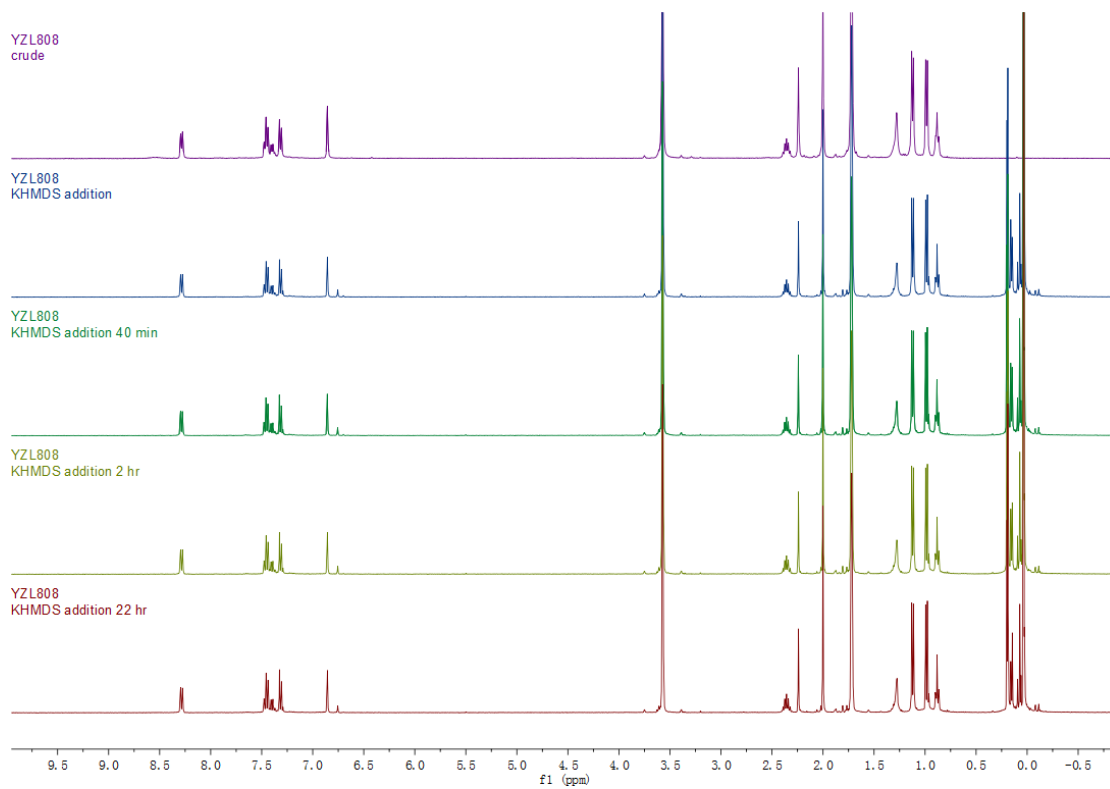


Figure S17 <sup>1</sup>H NMR spectra of **12** in THF-d<sub>8</sub> before and after addition of KHMDS at different times.

### 3. ESR Spectroscopy

The ESR measurements (**3** and **6**) were performed at room temperature using a Bruker EleXsys E500 X-band ESR spectrometer, which was equipped with a high-Q cylindrical cavity, Model ER 4122 SHQE (from Bruker BioSpin GmbH, Karlsruhe, Germany). The instrumental settings were: sweep width of 100 G; magnetic field modulation frequency 100 kHz; magnetic field modulation amplitude 0.05 G (0.005 mT); lock-in time constant 10.24 ms; lock-in integration time 40.96 ms; number of points per scan 2048; resulting sweeping time 83.89 sec; typical microwave frequency ~9.400 GHz; microwave power 0.6336 mW; number of scans accumulated per each spectrum 2. 2,2-Diphenyl-1-picrylhydrazyl (DPPH) was used as a reference sample to determine *g*-factor values.

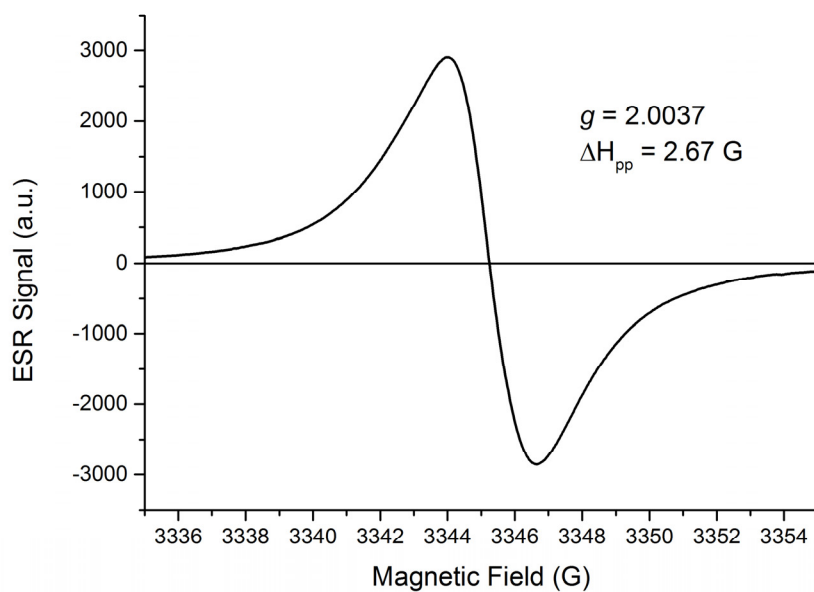


Figure S18 Solid-state ESR spectrum of **3** at RT.

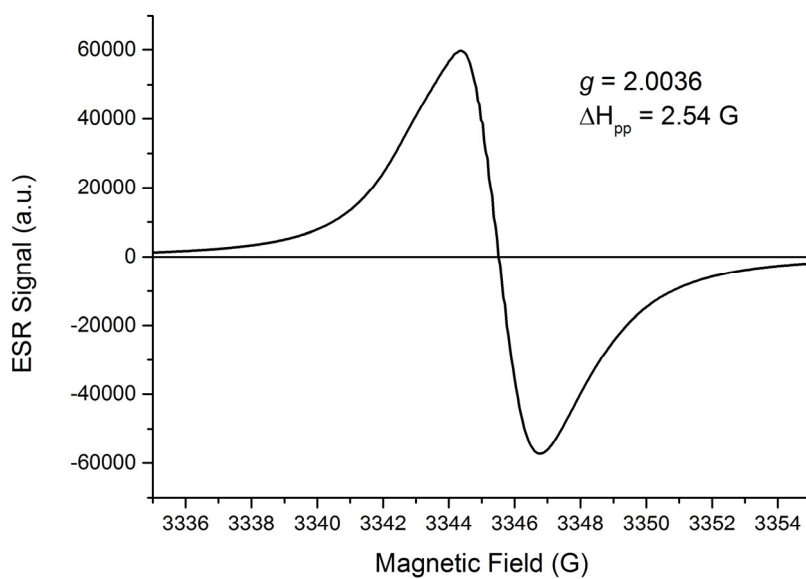


Figure S19 Solid-state ESR spectrum of **6** at RT.

#### 4. X-Ray crystallography

The diffraction data of all compounds were measured at low temperature using Cu  $K_{\alpha}$  radiation on a Rigaku SuperNova dual system in combination with Atlas type CCD detector. The data reduction was carried out - in all cases - by *CrysAlis<sup>Pro</sup>*.<sup>3</sup>

The solutions and refinements were performed by *SHELXT*<sup>4</sup> and *SHELXL*<sup>5</sup>, respectively. The crystal structures were refined using full-matrix least-squares based on  $F^2$  with all non hydrogen atoms anisotropically defined. Hydrogen atoms were placed in calculated positions by means of the “riding” model.

Additional electron density (due to disordered solvent molecules) found in the difference Fourier map of compound **3**, **4**, **6** and **11** was treated by the *SQUEEZE* algorithm of *PLATON*.<sup>68</sup> Pseudo merohedral twinning was found for compound **7** and treated directly by *CrysAlis<sup>Pro</sup>* <sup>3</sup> obtaining 1 BASF factor: 0.468(1). Similarity and rigid bond restraints (SIMU and SADI cards) were employed during the last stages of refinement of all structures except **4** because of the disorder displayed by the THF molecules.

Crystallographic data have been deposited to the CCDC and correspond to the codes CCDC1903893–1903897. Copies of the data can be obtained free of charge on application to the CCDC, 12 Union Road, Cambridge, CB2 1EZ, U.K. (fax, (internat.) +44-1223-336033; E-mail, deposit@ccdc.cam.ac.uk).

---

<sup>3</sup> *CrysAlis<sup>Pro</sup>*, Rigaku Oxford Diffraction, release 1.171.39.46, 2018.

<sup>4</sup> *SHELXT* - Integrated space-group and crystal-structure determination, G. M. Sheldrick, *Acta Crystallogr., Sect. A*, 2015, **71**, 3–8.

<sup>5</sup> *SHELXL* - Crystal structure refinement, G. M. Sheldrick, *Acta Crystallogr., Sect. C*, 2015, **71**, 3–8.

<sup>6</sup> *PLATON*, A. L. Spek, *Acta Crystallogr., Sect. D*, 2009, 65, 148–155.

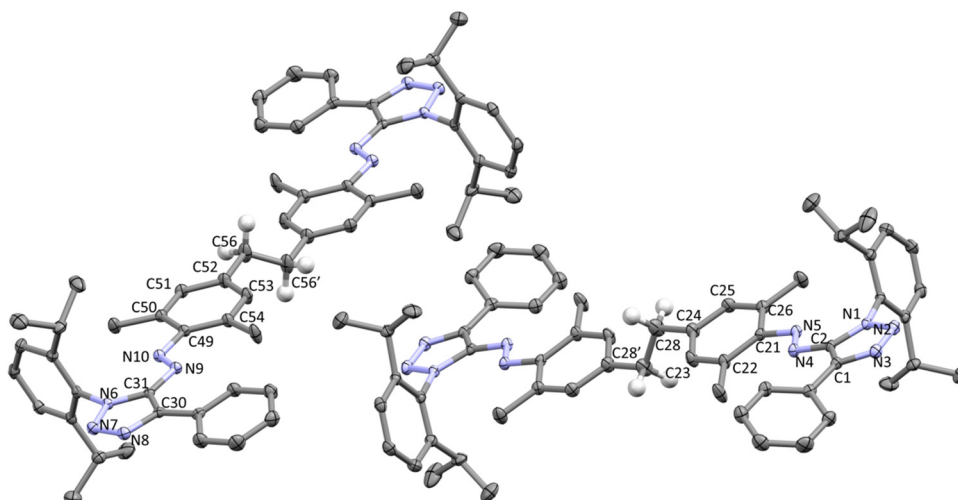


Figure S20 The crystal structure of **7**. The ellipsoids are shown at 30% probability. The unit cell contains two independent molecules, and both are shown here. Hydrogen atoms, except those on the ethylene bridge, and solvent molecules, are omitted for clarity. Selected bond lengths (Å) and bond angles (°): C28–C28' 1.443(5), C24–C28 1.504(3), C23–C24 1.397(3), C22–C23 1.386(2), C21–C22 1.420(2), C21–C26 1.414(2), C25–C26 1.387(2), C24–C25 1.387(3), C21–N5 1.410(2), N4–N5 1.265(2), N4–C2 1.395(2), C1–C2 1.392(2), C1–N3 1.359(2), N2–N3 1.309(2), N1–N2 1.351(2), N1–C2 1.370(2), C56–C56' 1.433(4), C52–C56 1.505(2), C51–C52 1.388(3), C50–C51 1.386(2), C49–C50 1.420(2), C49–C54 1.416(2), C53–C54 1.390(2), C52–C53 1.399(2), C49–N10 1.415(2), N9–N10 1.264(2), N9–C31 1.401(2), C30–C31 1.397(2), C30–N8 1.361(2), N7–N8 1.303(2), N6–N7 1.353(2), N6–C31 1.367(2), C24–C28–C28' 115.5(2), C21–N5–N4 117.0(1), N5–N4–C2 114.0(1), C52–C56–C56' 117.5(2), C49–N10–N9 117.9(1), N10–N9–C31 114.0(1).

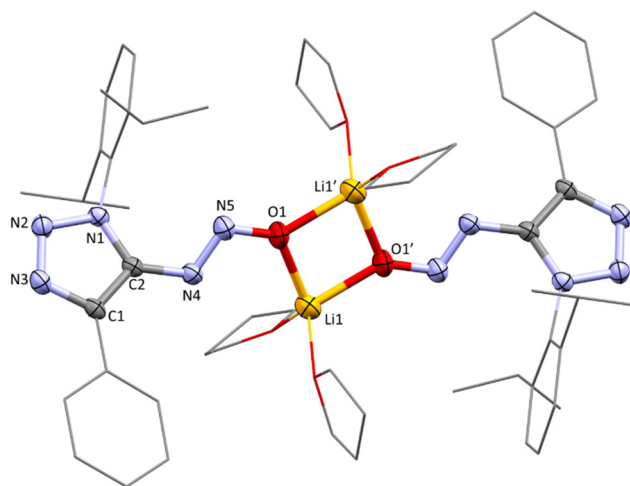


Figure S21 The crystal structure of **11**. The ellipsoids are shown at 30% probability. The unit cell contains two symmetry-related molecules. Hydrogen atoms are omitted for clarity. Selected bond lengths (Å) and bond angles (°): O1–Li1 1.928(4), O1–Li1' 1.937(4), N5–O1 1.289(2), N4–N5 1.263(2), C2–N4 1.392(2), C1–C2 1.387(2), C1–N3 1.358(2), N2–N3 1.304(2), N1–N2 1.362(2), N1–C2 1.357(2), Li1–O1–Li1' 96.4(2), O1–Li1–O1' 83.6(2), N5–O1–Li1 139.1(2), N4–N5–O1 112.2(2), C2–N4–N5 113.0(2).

## 5. Cyclic voltammetry of compound 4

The experiments were carried out under an atmosphere of dinitrogen in degassed and anhydrous acetonitrile solution containing TBAPF<sub>6</sub> (0.1 M) at a scan rate of 100 mV s<sup>-1</sup> up to 250 mV s<sup>-1</sup>. The setup consisted of a platinum working electrode (surface area = 0.06 cm<sup>2</sup>), a platinum wire as the counter electrode, and a silver wire immersed in a 0.01 M AgNO<sub>3</sub>/ 0.1M TBAPF<sub>6</sub> solution in dry acetonitrile. The voltammograms have been referenced to the external standard Fc/Fc<sup>+</sup> (ferrocene/ferrocenium) couple.

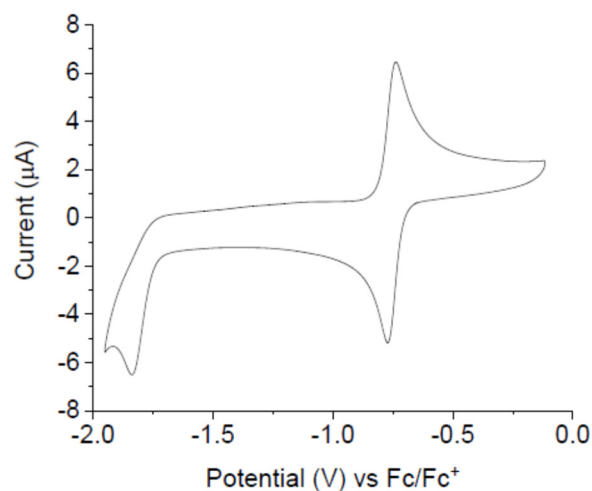


Figure S22 Cyclic voltammogram compound 4. WE and CE: Pt, RE: Ag/AgNO<sub>3</sub> 0.1M in MeCN, under N<sub>2</sub>, dry MeCN, scan rate: 100 mV s<sup>-1</sup>. Redox events are observed at E<sub>1/2</sub> = -0.76 V and -1.34 V (irreversible) vs. Fc<sup>+</sup>/Fc.

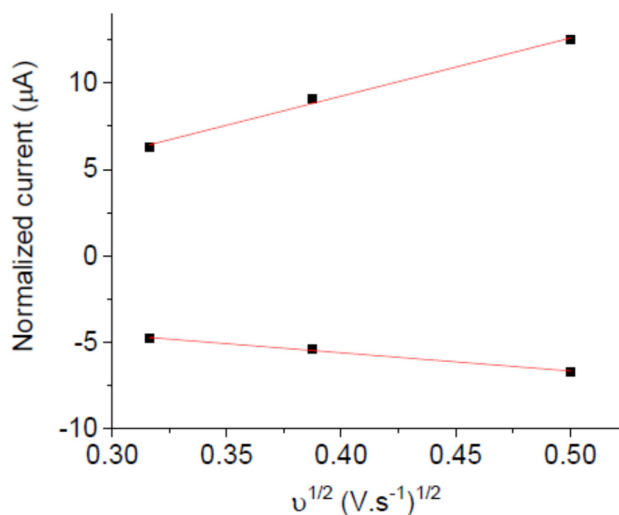


Figure S23 Reversibility of the wave at -0.76 V vs Fc<sup>+</sup>/Fc.

## 6. DFT Computations

All density functional theory computations were performed at the (U)TPSS<sup>7</sup>-D3<sup>8</sup>/cc-pVDZ level in Gaussian16.<sup>9</sup> Due to the intrinsic multiconfigurational nature of open-shell singlets, these states were treated within a broken-symmetry formalism. The validity of DFT results is, nevertheless, supported by the small and highly localized fractional occupancy density<sup>10</sup> (FOD), that characterizes the compounds analyzed (Figure S24). Therefore, semi-local functionals such as the chosen TPSS are well adapted to describe all the spin states treated in this work.<sup>9</sup>

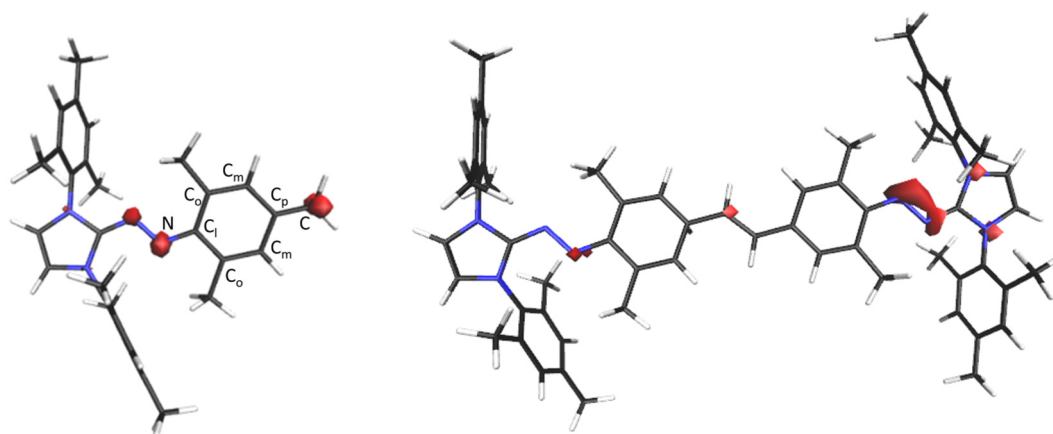


Figure S24. FOD plot of **2B** (left) and **4** (right). The FOD (in red) is plotted at the recommended isovalue of 0.005 e<sup>-</sup>/Bohr<sup>3</sup>.

Table S1 Comparison of the bond lengths (Å) of *p*-QDM and computed **2B**. Atom labels are specified in Figure S24.

	C–C <sub>p</sub>	Avg. C <sub>p</sub> –C <sub>m</sub>	Avg. C <sub>m</sub> –C <sub>o</sub>	Avg. C <sub>o</sub> –C <sub>l</sub>
<i>p</i> -QDM <sup>11</sup>	1.39	1.45	1.38	1.45
<b>2B</b>	1.37	1.45	1.37	1.47

<sup>7</sup> J. Tao, J. P. Perdew, V. N. Staverov and G. E. Scuseria, *Phys. Rev. Lett.*, 2003, **91**, 146401.

<sup>8</sup> S. Grimme, J. Anthony, S. Ehrlich and H. Krieg, *J. Chem. Phys.*, 2010, **132**, 154104.

<sup>9</sup> J. M. Frisch, G. W. Trucks, H.B. Schlegel, G.E. Scuseria, M.A. Robb, J.R. Cheeseman, G. Scalmani, V. Barone, G.A. Peterson and H. Nakatsuji, *et al.* Gaussian16 Revision B.01. 2016

<sup>10</sup> S. Grimme and A. Hansen, *Angew. Chem. Int. Ed.*, 2015, **54**, 12308–12313.

<sup>11</sup> P. G. Mahaffy, J. D. Wieser and L. K. Montgomery, *J. Am. Chem. Soc.*, 1977, **99**, 4514–4515.

The resonance structure of compound **4** can be described either as a closed-shell “quinoidal” form or as an open-shell diradical. For this reason, its X-ray structure was relaxed at (U)TPSS-D3/cc-pVDZ for the singlet closed-shell (CS), singlet open-shell (OS) and triplet (T) spin states. The singlet closed-shell state was found to be favored by 8.58 kcal/mol over the triplet state, while the open-shell singlet was only found as an electronically excited state, lying approximately 38.8 kcal/mol higher than the CS state (Table S2). From the structural perspective, the singlet CS state is the one that matches more closely the experimentally determined bond lengths and bond length alternation (BLA) (Table S3).

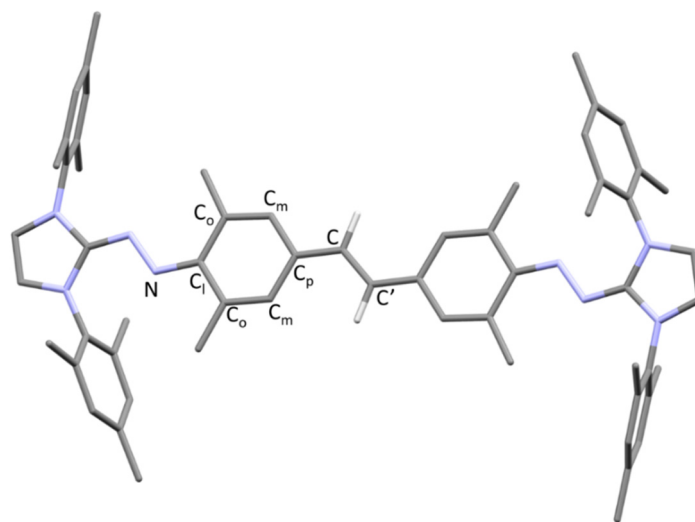


Figure S25. The optimized structure of **4**. Hydrogen atoms except those on the vinyl bridge are omitted for clarity.

Table S2. Experimental and computed bond lengths (Å), relative energies (kcal mol<sup>-1</sup>) and bond length alternation (BLA) for the X-Ray, closed-shell (CS), open-shell (OS) and triplet (T) states of molecule **4**.

Molecule <b>4</b>	$\Delta E$ [kcal/mol]	Avg. Co- Cm	Avg. Cm- Cp	Avg. Cl- Co	BLA [Benzene]	Avg. Cp- C	C-C'	BLA [Central]
CS	0	1.38	1.44	1.46	0.07	1.42	1.40	0.02
OS	38.77	1.39	1.42	1.45	0.045	1.45	1.38	0.07
T	8.59	1.39	1.42	1.45	0.045	1.46	1.37	0.09
cis-CS	3.24	1.38	1.44	1.46	0.07	1.42	1.41	0.01
cis-T	8.55	1.39	1.42	1.44	0.04	1.46	1.37	0.09
X-Ray	-	1.37	1.42	1.45	0.065	1.42	1.40	0.02

Table S3 Comparison of selected bond lengths of **3**, **4**, the computed version of **4**, and **TH** (Tschitschibabin's hydrocarbon). Atom labels are specified in Figure S25.

	<b>3</b>	<b>4 Exp</b>	<b>4 Computed</b>	<b>TH</b> <sup>12</sup>
C–C'	1.48	1.41	1.40	
C–C <sub>p</sub>	1.52	1.42	1.42	
C <sub>p</sub> –C <sub>m</sub> , avg.	1.39	1.42	1.44	1.42
C <sub>m</sub> –C <sub>o</sub> , avg.	1.39	1.37	1.38	1.37
C <sub>o</sub> –C <sub>l</sub> , avg.	1.42	1.45	1.46	1.43
BLA (mesitylene)	0.014	0.067	0.070	0.052
C <sub>l</sub> –N	1.39	1.34	1.35	

The X-ray structure of compound **6** was relaxed at (U)TPSS-D3/cc-pVDZ for the singlet closed-shell (CS), singlet open-shell (OS) and triplet (T) spin states. Singlet open-shell biradical and triplet were found to be almost isoenergetic and favored by 4.75 kcal/mol over the closed-shell singlet (Table S4).

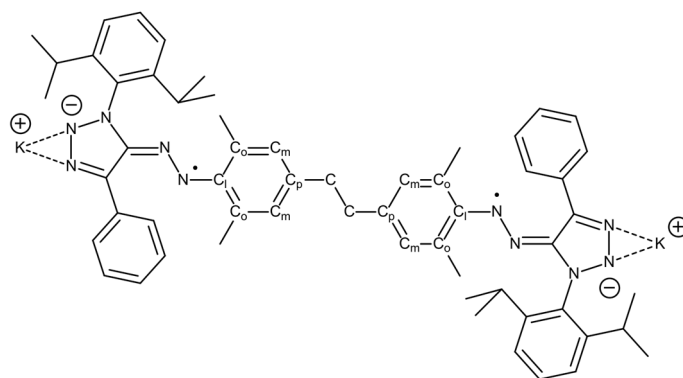


Table S4. Experimental and computed bond lengths (Å), relative energies (kcal mol<sup>-1</sup>) and bond length alternation (BLA) for the X-Ray, closed-shell (CS), open-shell (OS) and triplet (T) states of molecule **6**.

Molecule <b>6</b>	$\Delta E$ [kcal/mol]	Avg. Co- Cm	Avg. Cm- Cp	Avg. Cl- Co	BLA [Benzene]	Avg. Cp- C	C-C	BLA [Central]
CS	4.76	1.40	1.41	1.45	0.03	1.50	1.58	-0.08
OS	0	1.40	1.41	1.44	0.025	1.51	1.57	-0.06
T	0.15	1.40	1.41	1.44	0.025	1.51	1.56	-0.05
X-Ray	-	1.38	1.44	1.41	0.045	1.49	1.44	0.05

<sup>12</sup> L. K. Montgomery, J. C. Huffman, E. A. Jurczak and M. P. Grendze, *J. Am. Chem. Soc.*, 1986, **108**, 6004–6011.